Interactions of cyclodextrins and their hydroxyl derivatives with Etodolac: solubility and dissolution enhancement

Wesam W. Mustafa[1], Mouhamad Khoder[2], Hamdy Abdelkader[3,4], Richard Singer[5], Raid G. Alany[2,6]

[1] Department of Pharmacy, Al-Mustafa University College, Baghdad, Iraq

[2]Drug Discovery, Delivery and Patient Care Theme, Department of Pharmacy, Kingston University London, Kingston upon Thames, KT1 2EE, UK

[3]Department of Pharmaceutics, Faculty of Pharmacy, Minia University, Minia, Egypt

[4]Department of Pharmaceutics, College of Pharmacy, King Khalid University, Abha 61441, Aseer, Saudi Arabia

[5] Department of Chemical and Pharmaceutical Sciences, School of Life Sciences, Pharmacy and Chemistry, Kingston University London, Kingston upon Thames, KT1 2EE, UK

[6] School of Pharmacy, The University of Auckland, Auckland, New Zealand

Background: Poor solubility and dissolution rate of drugs are largely responsible for erratic drug absorption and limited oral bioavailability. Etodolac (ETO) is a non-steroidal anti-inflammatory drug (NSAID) that is classified as BCS class II (dissolution rate-dependent absorption). ETO has high safety and efficacy in pain relief and control of inflammation. ETO is commercially available as (400-600 mg) tablets; poor solubility and dissolution rate of ETO could result in variable oral absorption and inconsistent analgesic responses. The aim of this study was to improve solubility and dissolution rates of ETO by complexation with cyclodextrins (CDs).

Methods: Four different CDs namely β-, γ-, HP β-CDs and HP γ-CDs were prepared using three different methods; solvent evaporation (CO), freeze drying (FD) and physical mixting (PM). The prepared drug: excipient mixtures were investigated for aqueous solubility, as well as via DSC, XRD, FTIR, SEM, dissolution, and docking. **Results**: The results revealed a solubility phase diagram of the A_L type, indicating 1:1 complexation of ETO:CD. These results agreed with our molecular docking calculations. DSC, FTIR, XRD and SEM results confirmed the formation of an inclusion complex. The complexation efficiency, solubility and dissolution enhancement were in the order of: HPγ-CD > γ-CD > HPβ-CD > β-CD. FD method was superior to both CO and PM. **Conclusion**: Superior dissolution enhancements of ETO were recorded for FD mixture (up to 90% dissolved in less than 10 min). In conclusion, γ- and hydroxypropyl γ-derivative of cyclodextrins can be considered a promising excipient for enhancement of dissolution rates concerned for ETO.

1. Introduction

Etodolac (ETO) is a NSAID that can be indicated for management of mild to moderate pain such as that associated with osteoarthritis and rheumatoid arthritis. It is a pyrano-acetic acid derivative; chemical structure is shown in Figure 1. ETO has 10-fold COX 2 selectivity over COX 1; it works via inhibition of prostaglandins synthesis which is involved in inflammation, swelling fever, and pain (1, 2). ETO is marketed and administered as a racemic mixture. The (S)-enantiomer has been reported to be more potent than the (R)-enantiomer (3).

ETO is practically insoluble in water; its estimated log P values is 3.59 (ACD/Sketch 2017.1.2.). This indicates that ETO can be classified as Biopharmaceutics Classification Scheme (BCS) II drug; in other words it has high permeability and low solubility in the gastrointestinal tract (GIT) (4). Being a class II drug, the bioavailability of ETO will be controlled by its dissolution rate (5). Therefore, enhancement of ETO's solubility and dissolution rate will inevitably enhance its oral bioavailability (6, 7)

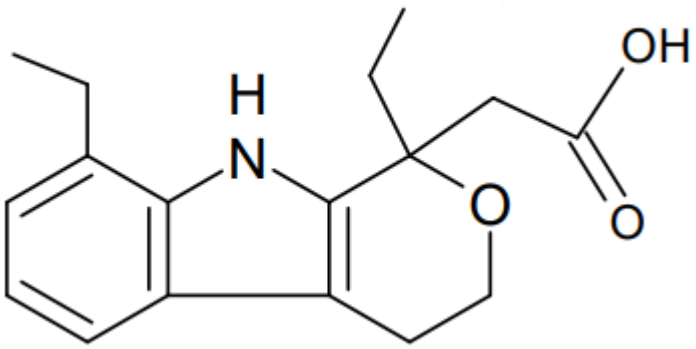

Fig. 1 Chemical structure of Etodolac

Different approaches have been reported to improve the solubility of poorly soluble drugs; They include: solid dispersions (8), reduction of particle size (9, 10), salt formation (11, 12), use of cosolvents (13, 14), surfactants (15, 16), amino acids (17), and other particle engineering techniques (18, 19).

Cyclodextrins (CD) are a group of cyclic oligosaccharides forming cyclic cavities of varying sizes based on the number of constituting sugar moieties: six for α-CD; seven for β- CD; and eight for γ-CD. They were originally discovered in 1890 (20, 21). The main feature of cyclodextrins is attributed to their ability to form an inclusion complex with a guest molecule (22-30). They possess a ring structure, with a hydrophobic inner cavity and external hydrophilic surface (31-36). The inner cavity can fit a guest molecule, while the outer surface is sufficiently hydrophilic to impart substantial water solubility (37). The formed complex alters the physiochemical characteristics of the guest, in particular to enhance water

solubility (38). Inclusion complexes with CDs have been successfully used for preparation of commercially available pharmaceuticals to enhance the solubility (39-42). Globally, there are more than 30 pharmaceutical products containing cyclodextrins. For example, Piroxicam is one of NSAIDS and is available commercially in a fast-dissolving piroxicam-cyclodextrin complex under the commercial name of Brexin® (43). Inclusion of NSAIDS in CD has resulted in numerous benefits such as improving solubility, dissolution rates, in vivo bioavailability, reducing gastric irritation and toxicity (44-46).

This manuscript reports on the formulation of ETO solid dispersions using CDs: β-, γ- and their hydroxy propyl (HP) derivatives, typically HPβ-CDs, and HPγ-CDs. Three preparation techniques including CO, FD and PM were employed. The prepared dispersed mixtures were characterized for equilibrium solubility, morphology using scanning electron microscopy (SEM), thermal behaviour using DSC, crystalline structure using X-ray powder diffraction (XPRD), dissolution and molecular interaction using FTIR spectroscopy to elucidate the complexation process. Molecular docking studies were conducted to calculate ETO:CD binding free energies to evaluate the stability of the formed complex.

2. Materials and Methods

2.1. Materials

ETO, β- and γ-were sourced from TCI, UK. Methanol, HP-β-CD and HP-γ-CD were sourced from Sigma-Aldrich, UK.

2.2. Solubility determination

Solubility of ETO in various molar concentrations of CD was studied at 25°C. Extra ETO was added to solutions with varying molar concentrations (0 to 20 mM) of β-, γ- HPβ-CD, and HPγ-CD and transferred into a shaking water bath adjusted at 25°C ± 0.5 and 100 ± 5 strokes per minute, shaken for 24h and then left for equilibrium for an additional 24h.

In addition, CD complex formulations and PM formulations were added in increased amount to 1 ml deionised water to make a final concentration of CDs of that mentioned above (47). Samples were withdrawn and filtered through 0.45μm filters. ETO concentrations were determined after appropriate dilution spectrophotometrically (Jenway, Staffordshire, UK) at 278 nm. The solubility constant (K) was calculated from the regression straight line of solubility versus cyclodextrin concertation plots using equation 1:

$$K = \frac{Slope}{So\ (1-slope)} \qquad equation\ 1$$

Where So is the solubility of ETO at cyclodextrin concertation = 0.

ETO-CDs solubility phase diagrams generated A_L type (linear) profiles where the complexation efficiency (CE) was calculated from equation 2 (47):

$$CE = S_o\ .K = \frac{Slope}{(1-Slope)} \qquad equation\ 2$$

2.3. Preparation of ETO-CD mixtures with the coprecipitation technique

Specified amounts of ETO and various forms of CDs (β-, γ-, HPβ-CD, and HPγ-CD) weighed and dissolved separately in methanol (50 ml) and water (50 ml) respectively at a molar ratio of 1:1. In a fume hood, the two prepared solutions were combined and magnetically stirred for 24 hours to allow solvent evaporation. The resultant solid particles were kept in a desiccator containing silica gel overnight to eliminate any residual moisture. The produced solid complexes were ground into powders and kept in hermetically sealed vials for future studies.

2.4. Preparation of ETO-CD solid dispersion using freeze drying technique

In a fume hood, the generated ETO-CD complexes were dissolved in 40 ml of deionized water and swirled magnetically for 30 minutes. The resultant solutions were then filtered, promptly frozen in liquid nitrogen and dried for a total of 72 hours using a VirTis Bench Top Freeze Dryer, UK.

2.5. ETO-CD physical mixture preparation

Accurately weighed amounts in mg of a 1:1 molar ratio of ETO and various CDs (β-, γ-, HPβ-CD, and HPγ-CD) were mixed for 10 minutes in a porcelain dish using a spatula.

2.6. Differential scanning calorimetry (DSC)

ETO, all types of cyclodextrins, their complexes, and PM were thermally assessed using the DSC, Mettler-Toledo Ltd. UK. The weighed sample (4-8 mg) was placed into a sealed aluminum crucible pan with pinholes under a 10 ml min^{-1} nitrogen. The samples were examined with STAReSW 10.00 software at 10°C/min from 25 to 450 °C.

2.7. X-ray Diffractometry (XRD)

Using a sophisticated X-ray diffractometer (BrukerAXS D8, Karlsruhe, Germany), the influence of inclusion complex formation on the crystallinity of ETO was examined. The instrument functioned at 45 kV and 40 mA current at room temperature. Samples of powder were scanned over the range 4–50° 2θ with a step size of 0.1. Using DIFFRAC plus XRD commander software, the produced X-ray powder diffractometers were examined.

2.8. Scanning electron microscopy (SEM)

A Carl Zeiss scanning electron microscopy (SEM) system (A Zeiss EVO 50, Oberkochen, Germany) was used to study the morphology of all ETO formulations. Samples were coated with gold using a sputter coater at 20 mA for 3 minutes prior to imaging (Polaron Equipment, Watford, UK). Using a sputter coater (Polaron Equipment, UK) and an argon atmosphere, powdered samples (formulations) were coated with gold for two to three minutes under vacuum in an argon atmosphere. The samples were then analysed by SEM at an acceleration voltage of 30 kV and low vacuum.

2.9. Fourier Transform Infrared (FT-IR) Spectroscopy

The diamond portion of the Thermo Fisher Scientific FTIR spectrometer (Nicolet iS5, iD5 advanced attenuated total reflectance (ATR, USA) was covered with 3-6 mg of powder samples. The data was collected and analysed. Each spectrum was collected with an average of 32 scans, a scanning range of 4000 cm^{-1} to 600 cm^{-1}, and a spectral resolution of 2 cm^{-1}.

2.10. Dissolution studies

Pure ETO, complexes, and PM were subjected to in vitro dissolution using the dissolution apparatus 2 (Caleva, UK). This experiment was run in 0.9 L consisting of 0.1 M HCl at 37 ± 1 ^{o}C and 100 rpm. The pure drug, the produced complexes, and PM powders (equal to 15 mg of pure drug) were mixed in the dissolving medium, and 2 ml aliquots were removed. The samples were filtered through 0.45 m Millipore filters before being scanned at 278 nm using a UV spectrophotometer (Jenway, Staffordshire, UK).

2.11. Molecular docking

To develop better understandings of ETO-CD complex formation with β-CD, γ-CD, HPβ-CD, and HPγ-CD, molecular docking was performed using AutoDock Vina (48). The 3D structures of CDs were obtained from Chemspider: β-CD (ChemSpider ID: 10469496), and γ-CD (ChemSpider ID: 10469499). Due to the lack of 3D structures for HPβ-CD, and HPγ-CD, the 3D structures of β-CD and γ-CD were utilised to construct the 3D structures of HPβ-CD and HPγ-CD using the software (Scigres, Fujitsu, Poland) by attaching manually an isopropyl group to the OH group of the glucopyranose ring (49). The 3D structure of ETO was retrieved from Chemspider: ETO (ChemSpider ID: 3192). The resulting binding energies between the ETO and CDs were calculated.

2.12. Statistical analysis

Analysis of variance (ANOVA) was used to establish the significance in the differences between the results at 95% CI ($p<0.05$) using graph prism software.

3. Results and Discussion

3.1. Solubility studies

To examine the effects of CDs on the solubility of ETO and study the complexation between ETO and various CDs, equilibrium solubility studies of ETO were conducted with excess amounts of CDs. Below are those results:

3.1.1. ETO-CDs Complexation

Figure 2 (a), Figure 3 (a), Figure 4 (a) and Figure 5 (a) represent bar graphs of ETO solubility for drug alone, PM and CO dispersions respectively. The solubility of ETO markedly increased from 57 mg/L to up to 300 mg/L. This is due to presence of CD that formed inclusion complexes, enhanced wettability of ETO and solubility. The ranking of solubilizing capacity of CDs used was as follows: HP γ-CD > γ-CD > HP β-CD > β-CD. The solubility enhancement was evidently dependent on both the type of CDs and the method of preparation. The used CDs have different inherent solubility in water: β-CD, γ-CD, HP-β-CD and HP-γ-CD have solubility of 18.5, 232, > 600 and > 500 mg/ml, respectively. It was evident that the higher the solubility of the used CD, the greater was its ETO solubilizing capacity.

Further, different CDs have different cavity sizes and hence affect ETO-CD complex-forming efficiency (CE) and solubility constant in water (47). The greater the solubility constant and CE of ETO-CD complex (Table 1); the higher was the solubility. For example, superior solubility of ETO from coprecipitated HPγ-CD and γ-CD complexes was attributed for having the highest solubility constant (193 and 173 M^{-1}) and CE (0.042 and 0.04), respectively. In addition, the preparation technique had a marked effect on CE and solubility of ETO. Coprecipitated mixtures demonstrated greater CE and higher solubility than PM counterparts. Dissolving the drug with the carriers (CD) and then co-evaporation of the solvent resulted in smaller drug particle sizes and allowed better contact between ETO and CD's cavity (17).

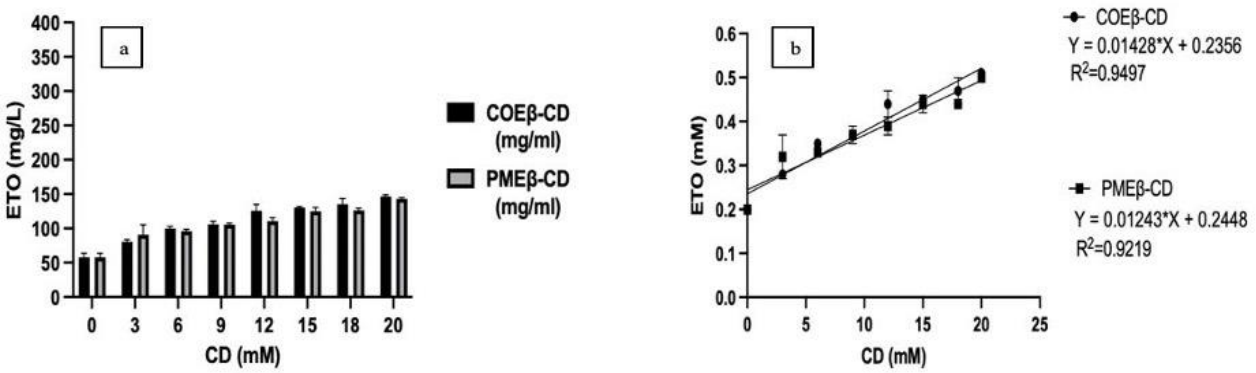

Fig 2. (a) ETO solubility versus β-CD concentrations, it's complexation (CO) and physical mixture (PM) formulations and (b) ETO/β-CD phase solubility diagrams of complexation (CO) and physical mixture (PM) (mean ± SD; n=3).

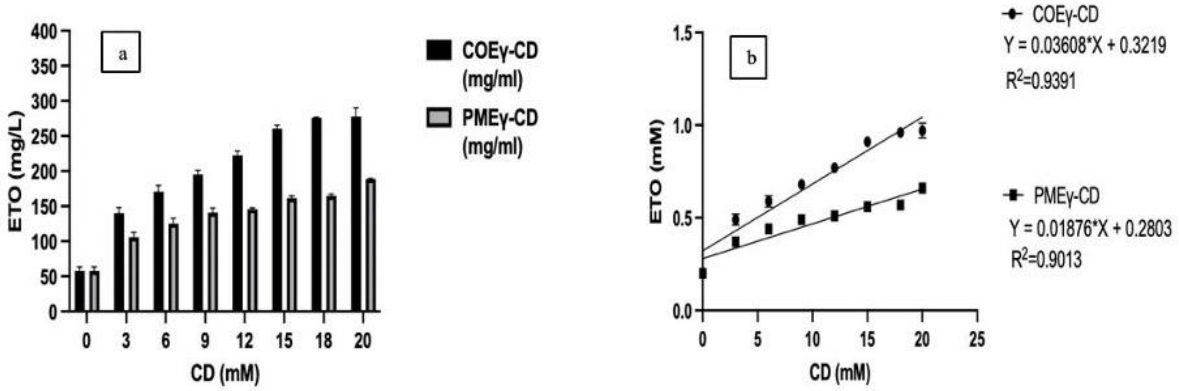

Fig 3. (a) ETO solubility versus γ-CD concentration (mM), it's complexation (CO) and physical mixture (PM) formulations and (b) ETO/ γ-CD phase solubility diagrams of complexation (CO) and physical mixture (PM) (mean ± SD; n=3).

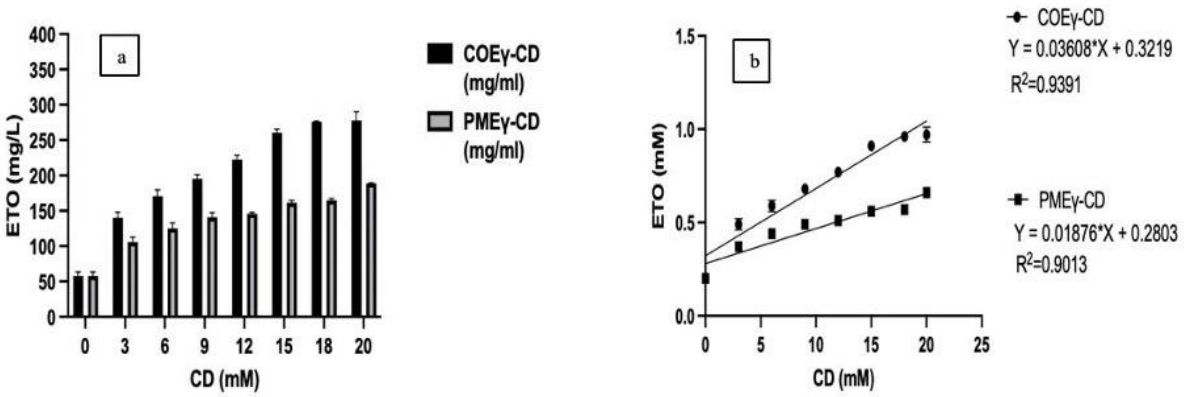

Fig 4. (a) ETO solubility versus HP-β-CD concentration (mM), it's complexation (CO) and physical mixture (PM) formulations and (b) ETO/ HP-β-CD phase solubility diagrams of complexation (CO) and physical mixture (PM) (mean ± SD; n=3).

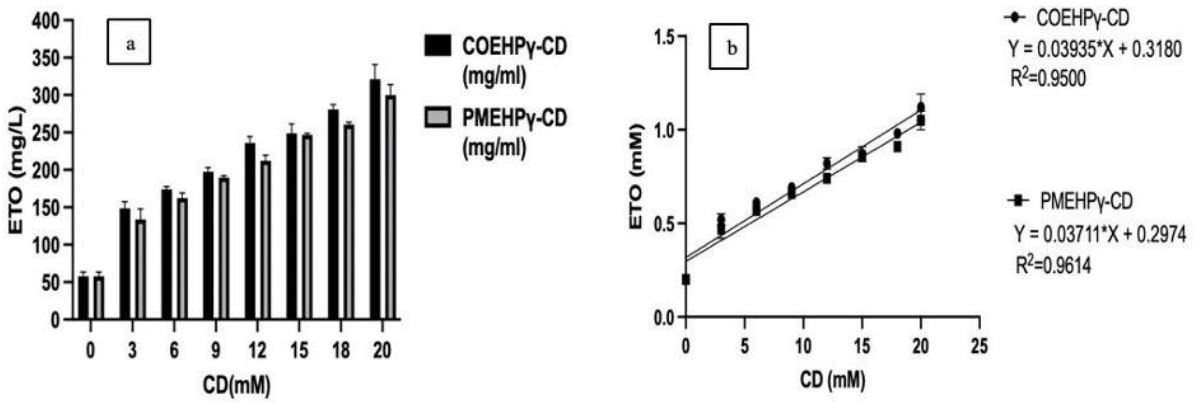

Fig 5. (a) ETO solubility versus the HP-γ-CD concentration (mM), it's complexation (CO) and physical mixture (PM) formulations and (b) ETO/ HP-γ-CD phase solubility diagrams of complexation (CO) and physical mixture (PM) (mean ± SD; n.3).

Figure 2 (b) Figure 3 (b), Figure 4 (b) and Figure 5 (b) shows phase solubility graphs of ETO. Linear relationship (A_L type) between solubility and CD concentrations indicating formation of complex (1:1). The solubility constant (K) and complexation efficiency (CE) were estimated for each ETO-CD PM and CO mixtures (Table 1). Both K and CE were in the order of: HP γ-CD > γ-CD > HP β-CD > β-CD. These results correlated well with the solubility studies. The greater the values of K and CE, the higher the solubility of ETO; this is due to formation of more stable host-guest complexes. It is worth mentioning that the preparation technique showed significant ($P < 0.05$) differences to enhance the complexation efficiency. For example, K and C for ETO: HPβ-CD COPPT were 1.5-fold greater than those recorded for the ETO: HPβ-CD PM.

ETO:CD	Preparation technique	K (M^{-1})	CE
ETO:β-CD	PM	61	0.013
	COPPT	71	0.015
ETO:γ-CD	PM	93	0.02
	COPPT	173*	0.04
ETO:HPβ-CD	PM	98*	0.02
	COPPT	146*	0.031
ETO:HP γ-CD	PM	178*	0.038
	COPPT	193*	0.042

Table 1: Effect of cyclodextrin type and preparation method on solubility constant (K) and complexation efficiency (CE)

3.2. Complexation, freeze drier and physical mixture characterisation

3.2.1. DSC

DSC provides information regarding solid interactions between ETO and CDs. (50). Figures 6 and 7 illustrate the DSC thermograms of pure, CO, FD, and PM components. The crystalline nature of ETO is shown by the presence of a prominent endothermic peak around 150 °C, which corresponds to its melting temperature (51). The β-CD, HP β-CD, and HP γ-CD thermograms exhibit very large endothermic peaks in the 25-140 °C range, which are ascribed to the removal of water (52). DSC Thermogram of γ-CD shows a melting peak at 160 °C (53). The same endothermic peaks for ETO were also observed in PM and in complex prepared by CO method but with less intensity comparing to the PM due to the little interaction which still indicating the crystal of the drug. However, ETO endothermic peak completely disappeared for the FD complex suggesting the drug dispersed completely in to the cyclodextrin to from amorphous dispersions.

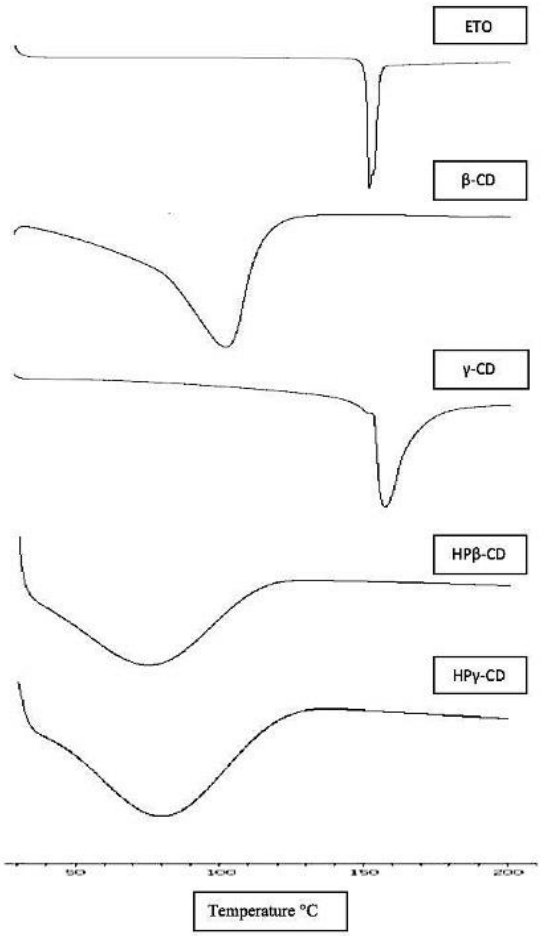

Fig.6. DSC thermogram of ETO raw material, ad CDs

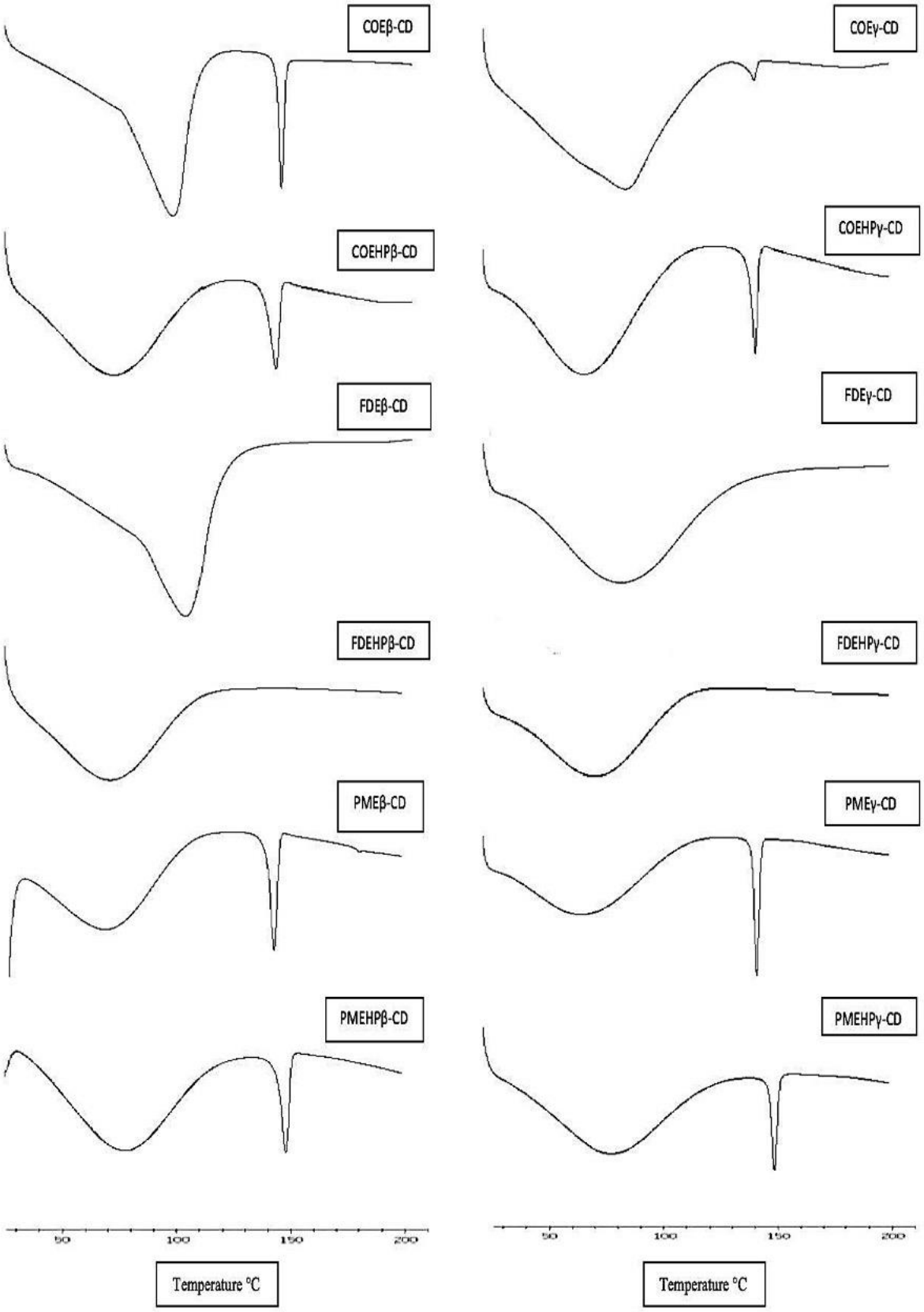

Fig. 7. DSC thermogram ETO as a complexation, solid dispersion, and physical mixture

3.2.2. XRD

The XRD diffractograms for ETO and cyclodextrin are shown in Figure 8. While the XRD diffractograms of the produced formulations via CO method, FD and PM are shown in Figure 9. The XRD diffractograms of ETO, β-CD, and γ-CD revealed several high-intensity shape packs confirming its crystalline form (1, 2). While HPβ-CD, and HPγ-CD diffractograms indicated the formation of amorphous mixtures. Similar distinctive peaks were seen in the XRD diffractogram of the PM prepared compound, and with less intensity for complex prepared by CO method which indicating minimum interaction (49). However, these distinctive peaks have disappeared entirely from the FD samples. In terms of complex formation, the XRD results are in good agreement with the DSC data.

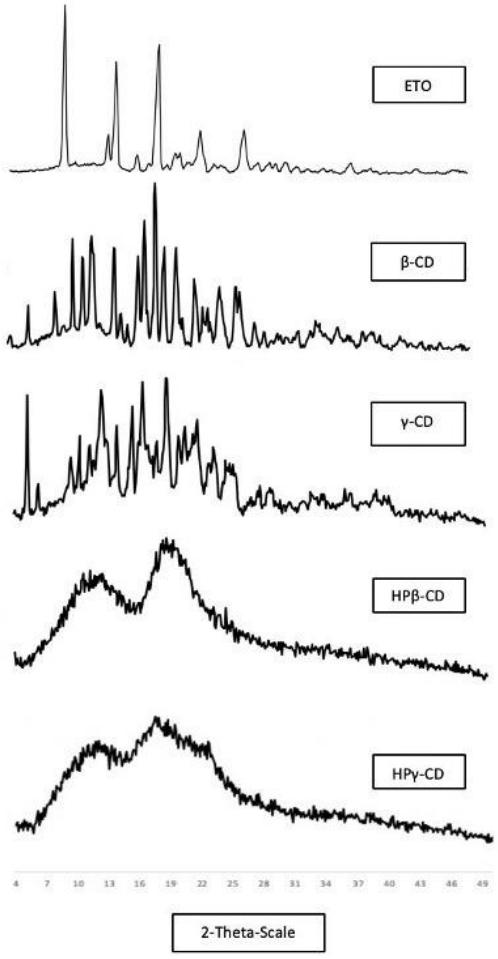

Fig.8. X-ray powder diffraction spectra of ETO raw material, ad CDs

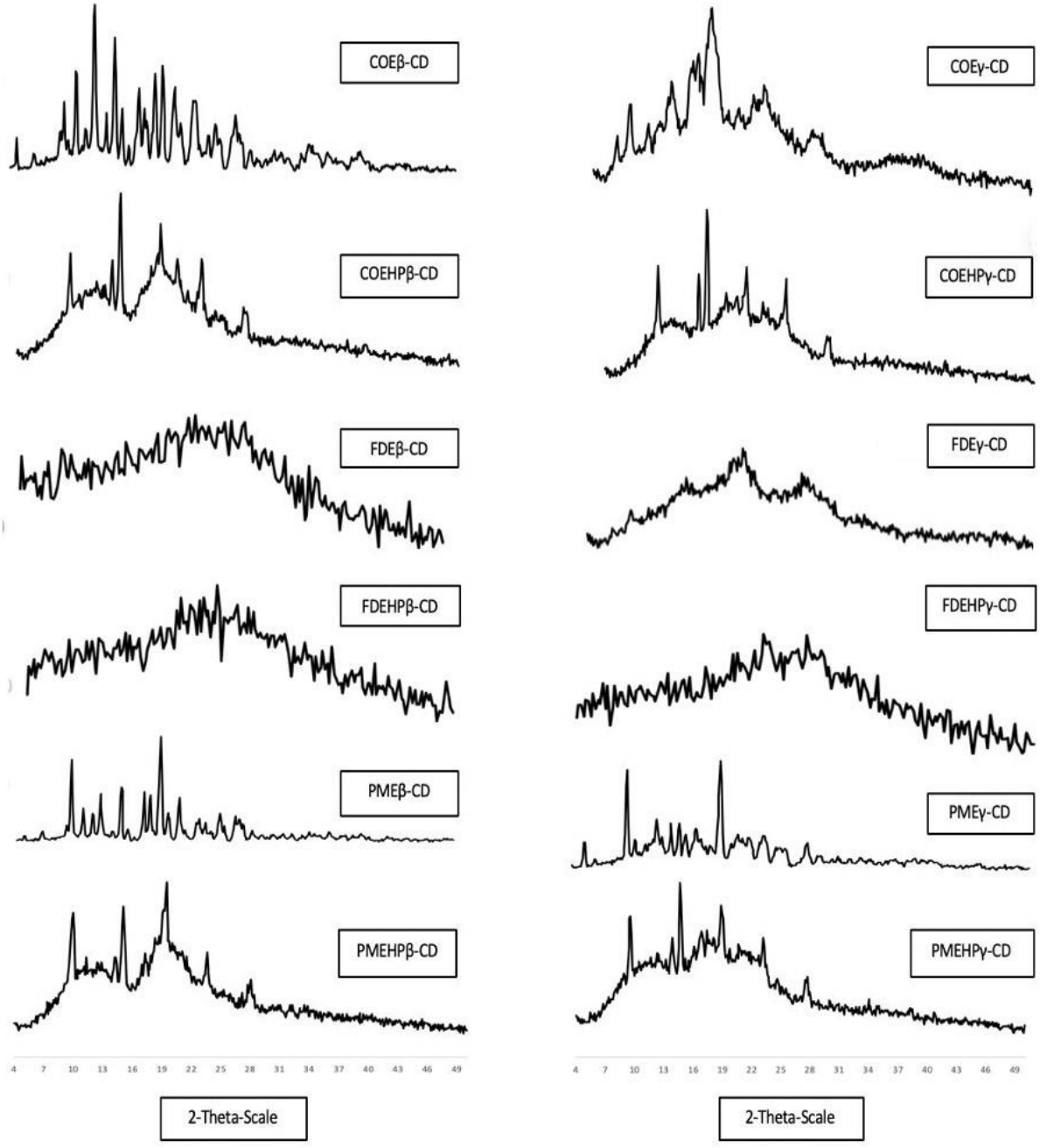

Fig. 9. X-ray powder diffraction spectra of ETO as a complexation, solid dispersion and physical mixture

3.2.3. SEM

The surface morphology of raw materials, CO, FD and PM obtained were examined using SEM (Figures 10 and 11). The PM images reveal no change in crystallinity or reduction of particle size. While the complexes prepared by FD and CO shows change in the morphology and reduction in particle size, suggesting possible molecular interaction between ETO and CD (54). The advantageous morphology and dimensions of FD formulations contribute to the greater surface areas subjected to the dissolution media and, as a result, are expected to have a major effect and enhance the dissolution rate of ETO from FD mixtures.

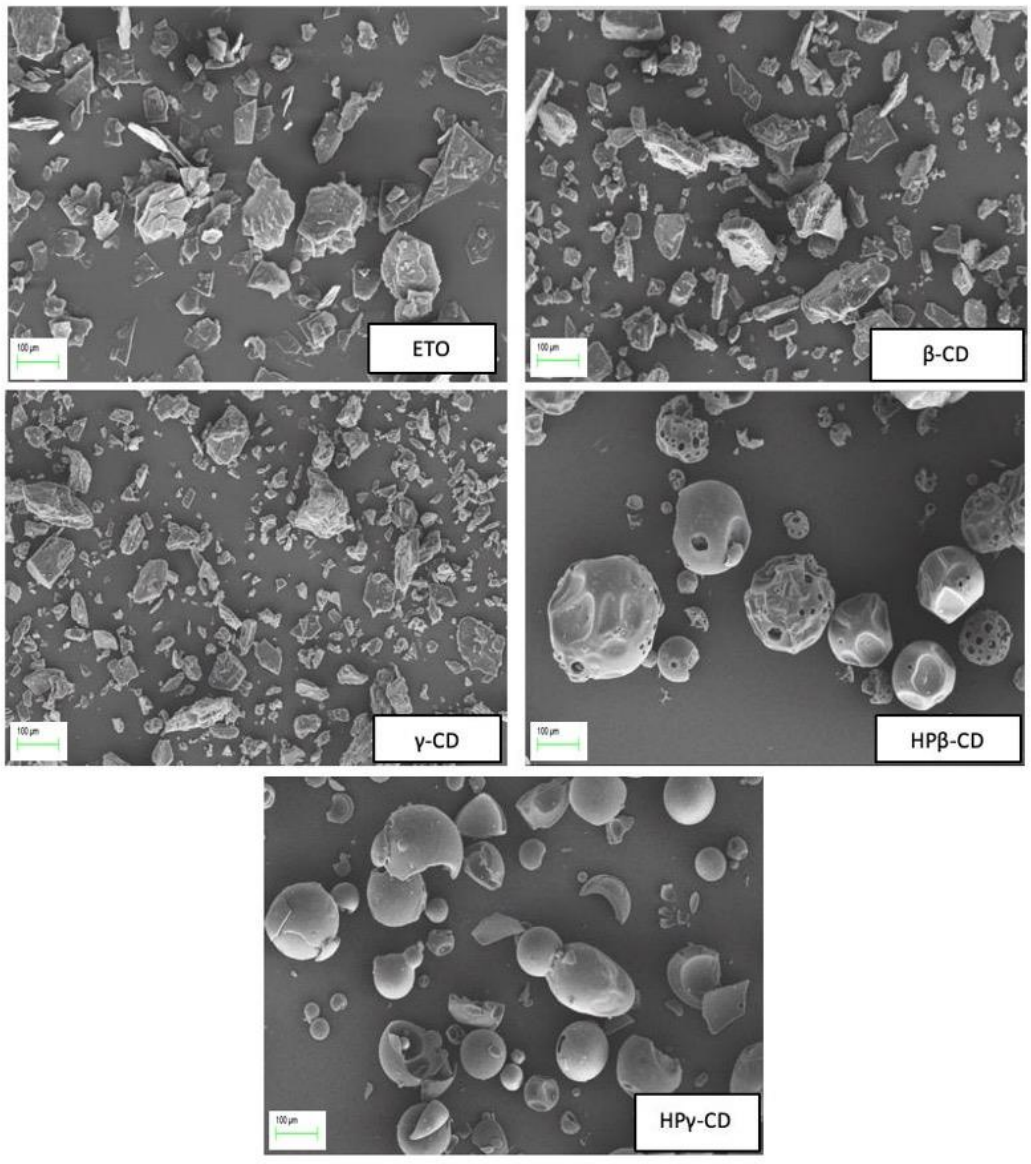

Fig.10. Representative SEM images of ETO raw material, ad CDs (scale bar 100µm)

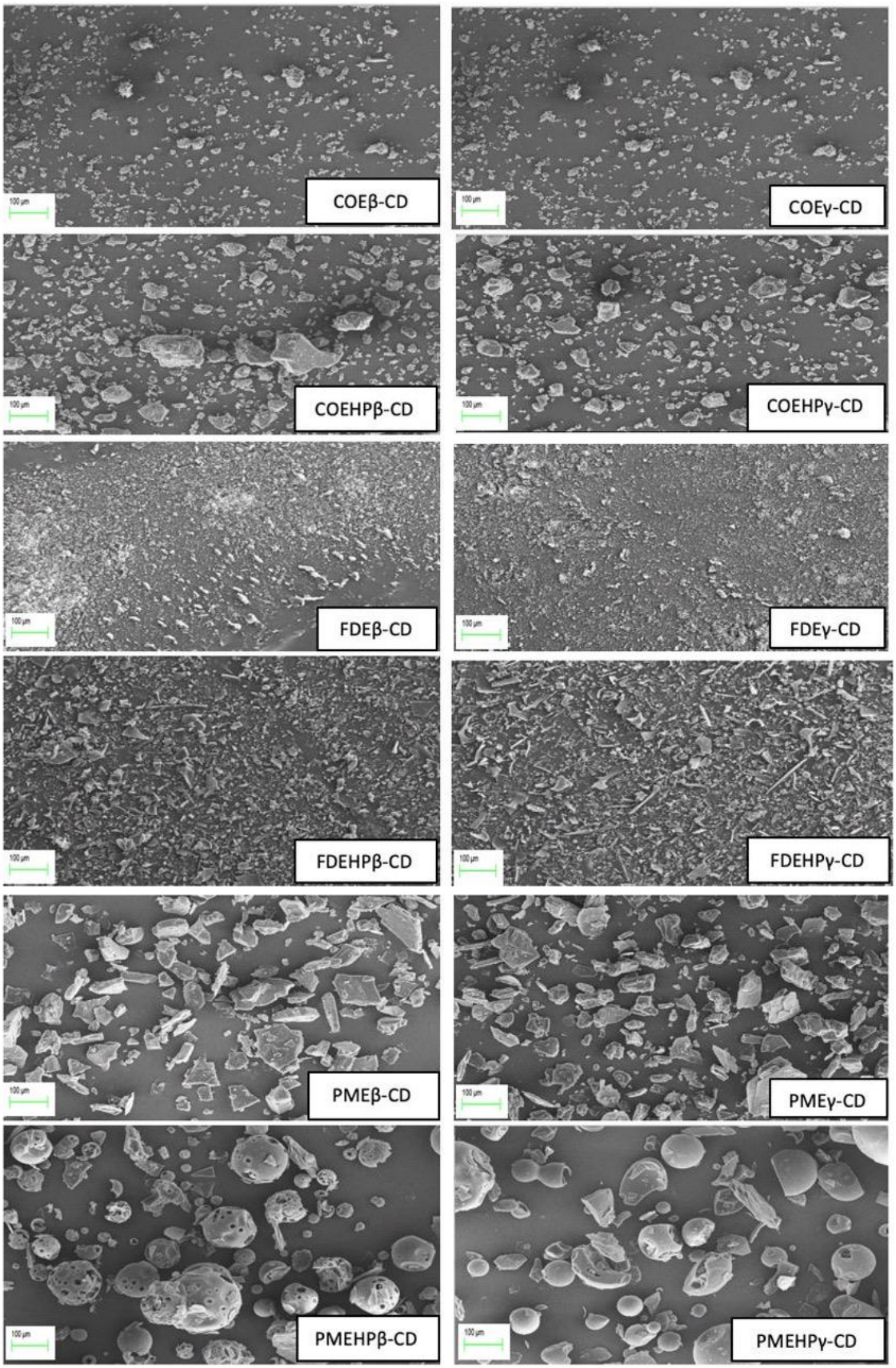

Fig. 11: Representative SEM images of ETO as a complexation, freeze dried and physical mixture (scale bar 100µm)

3.2.4. Infrared spectroscopy

-NH stretch, -CH stretch, -CO stretch, −CH bend, and -CN stretch peaks were seen in the IR spectrum of pure drug at 3345, 2972, 1746, 1412, and 1034 cm1, respectively. Figure12.a show that the IR spectrum of cyclodextrins revealed absorption bands at 3398 cm^{-1} (OH, stretch), 2924 cm^{-1} (CH, stretch), and 1025 cm^{-1} (C−O−C stretch). IR spectra of the mixtures prepared by CO and FD method showed clear changes in the characteristic absorption peaks for ETO as shown in Figure 12.b and c. In the formed complexes the intensity of characteristic absorption band was clearly reduced for ETO. The N−H stretch of ETO in the IR spectrum of FD complex was found completely flatten, compared to the complex prepared by CO and PM method which shows reduced in the intensity. Which reviles a good interaction between ETO and CD prepared by FD. The complex prepared by PM method (Fig. 12.c) showed less interaction of ETO with the cyclodextrins compared to the mixture prepared by CO and FD techniques as shown by characteristic peaks with less intensity observed in that complex. Thus, the flattening, broadening, and removal of the conspicuous peaks indicate the creation of complex formation that improves solubility.

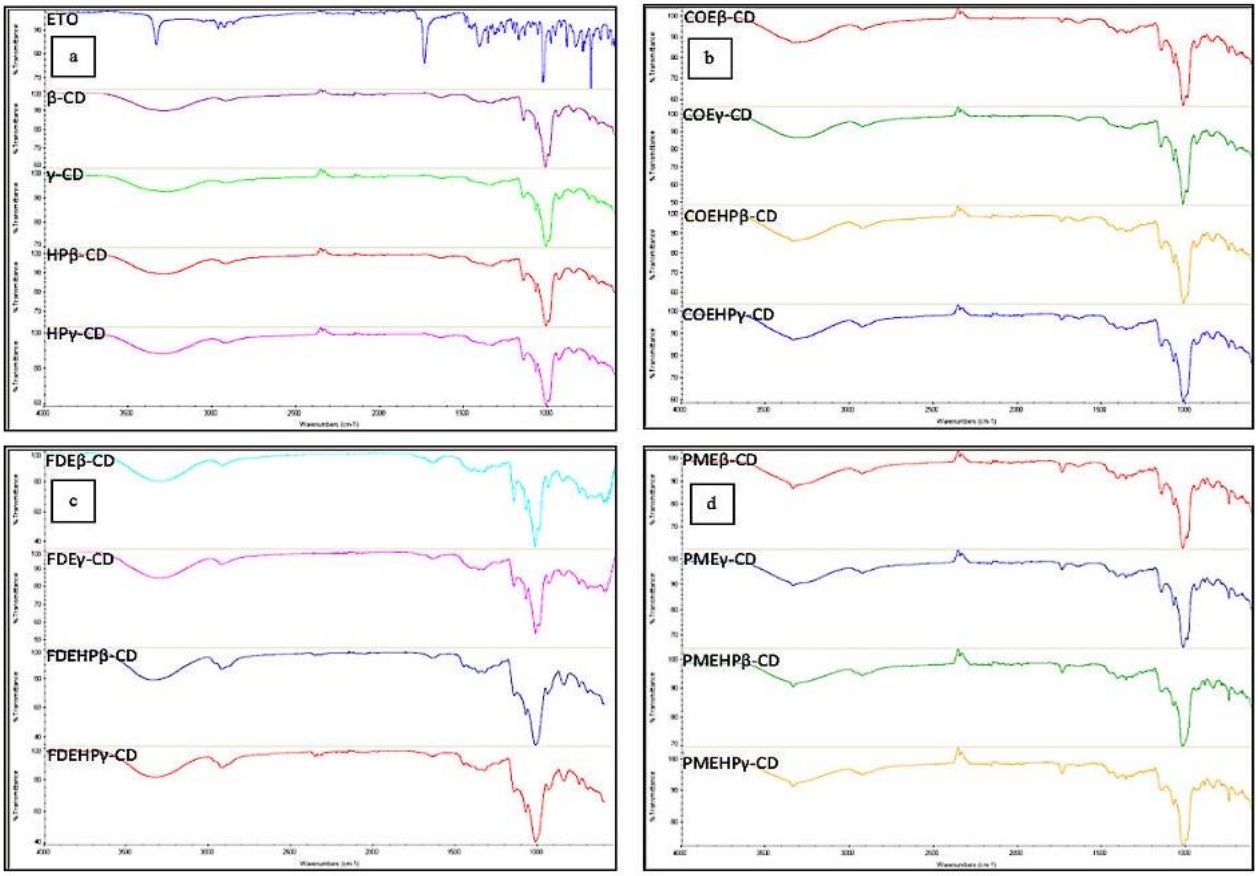

Fig. 12 a) AT-IR spectra of ETO raw material, β-CD, γ-CD, HP β-CD, and HP γ-CD. (b) Shows the AT-IR spectra of complexation of β-CD, γ-CD, HP β-CD, and HP γ-CD. (c) Shows the AT-IR spectra of Freeze drier of β-CD, γ-CD, HP β-CD, and HP γ-CD. (d) Shows the AT-IR spectra of physical mixture of β-CD, γ-CD, HP β-CD, and HP γ-C

3.2.5. Dissolution studies

Fig. 13 shows the dissolution profiles of ETO (pure drug) in a dissolution medium composed of pH 1.2 buffer at 37 °C. Being a weak acid (pKa 4.65), the dissolution rate in gastric pH 1.2 is particularly important to foresee the in vivo performance. The first part of the GIT is where ETO is likely to be mostly (unionised), hence available to be absorbed. The dissolution of ETO alone was relatively slow; a small fraction (approximately 10%) of ETO was dissolved in 60 min. Slight improving of dissolution was observed with ETO-CD PM (Figure 13b); while ETO-CD (Figure 13 c) prepared by FD showed the fastest dissolution rate (up to 90% of ETO dissolved in 10 min) compared with both ETO-CD PM (Figure 13b); and ETO-CD CO (Figure 13a). The reduction of particle sizes, increasing porosity of ETO, enhancement of solubility and inclusion complexation were the main reasons for explaining the significant enhancement of the dissolution of FD ETO-CD. The dissolution enhancement due to CD complexation was in the same ordered of binding and solubility constants: HPγ-CD > γ-CD > HPβ-CD >β-CD.

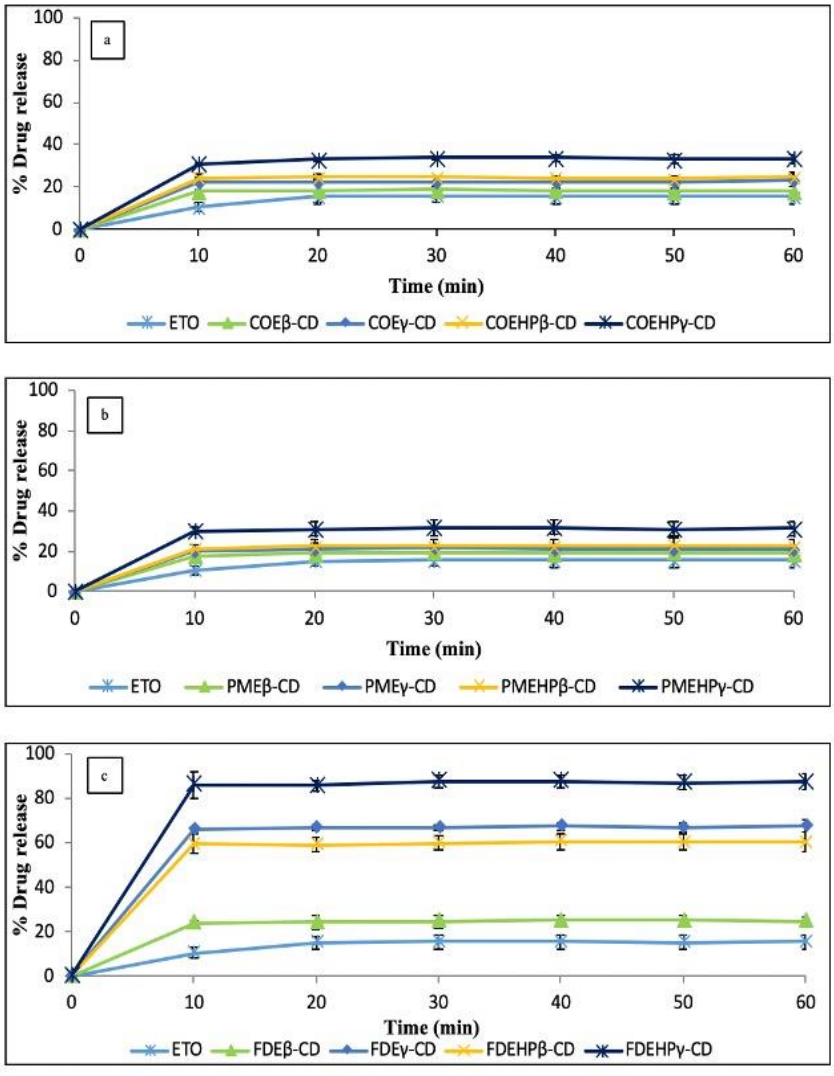

Fig. 13 In vitro dissolution profiles of ETO and ETO- β-CD, -γ-CD, -HP-β-CD, and -HP-γ-CD in pH 1.2 CO (a), ETO- β-CD, -γ-CD, -HP-β-CD, and -HP-γ-CD PM in pH 1.2 (b), ETO- β-CD, -γ-CD, -HP-β-CD, and -HP-γ-CD in pH 1.2 FD (c).

3.2.6. Molecular Docking

The calculated binding free energies for ETO-, HPβ-, γ-, and HP γ-CD are presented in Table 2. The ranking of binding forces between ETO-CDs was in the following descending order: HP γ-CD > γ-CD > HP β-CD > β-CD. The estimated binding free energy were broadly consistent with the trends in K and CE in Table 1. The greater the value the stronger the binding forces between host (CD)-guest (drug) complexes. COEHP γ-CD recorded highest value indicating strong binding. On the contrary, COEβ-CD showed lowest value.

Table 2. Binding constants for the prepared ETO-CD complexes

Complexes	Binding free energy (kcal/mol)
COEβ-CD	-5.7
COEγ-CD	-5.9
COEHPβ-CD	-5.8
COEHPγ-CD	-6.9

5. Conclusion

This study provided evidence on the role of CD on solubilization and enhancement of dissolution rate of ETO. Phase solubility diagrams indicated A_L type (1:1 complexation). The solubility constant ($K_{1:1}$) ranged from 61-193 M^{-1}. The estimated parameters were in good correlation with the docking calculation. Different preparation techniques were studied. The FD method seems to be superior over PM and co-evaporation methods. ETO-CD FD mixtures showed lower particle size, superior solubility and dissolution rate enhancement. These results warrant the use of CDs as potential excipients to produce a fast-dissolving dosage form of the analgesic drug ETO and future studies will look into evaluating gastric safety of ETO-CD compared to the drug alone.

References

1. Ammar H, Ghorab M, Mostafa D, Makram T, Ali R. Host–guest system of etodolac in native and modified β-cyclodextrins: preparation and physicochemical characterization. Journal of Inclusion Phenomena and Macrocyclic Chemistry. 2013;77(1-4):121-34.
2. Ibrahim MM, Mohamed E-N, El-Setouhy DA, Fadlalla MA. Polymeric surfactant based etodolac chewable tablets: formulation and in vivo evaluation. Aaps Pharmscitech. 2010;11(4):1730-7.
3. Demerson CA, Humber LG, Abraham NA, Schilling G, Martel RR, Pace-Asciak C. Resolution of etodolac and antiinflammatory and prostaglandin synthetase inhibiting properties of the enantiomers. Journal of medicinal chemistry. 1983;26(12):1778-80.
4. Aungst BJ. Novel formulation strategies for improving oral bioavailability of drugs with poor membrane permeation or presystemic metabolism. Journal of pharmaceutical sciences. 1993;82(10):979-87.
5. Serajuddin AT. Solid dispersion of poorly water-soluble drugs: Early promises, subsequent problems, and recent breakthroughs. Journal of pharmaceutical sciences. 1999;88(10):1058-66.
6. Rouchotas C, Cassidy O, Rowley G. Comparison of surface modification and solid dispersion techniques for drug dissolution. International journal of pharmaceutics. 2000;195(1-2):1-6.
7. Homdrum E-M, Likar R, Nell G. Xefo® rapid: a novel effective tool for pain treatment. European surgery. 2006;38(5):342-52.
8. Mustafa W, Fletcher J, Khoder M, Alany RG. Solid dispersions of gefitinib prepared by spray drying with improved mucoadhesive and drug dissolution properties. AAPS PharmSciTech. 2021.
9. Rasenack N, Müller BW. Dissolution rate enhancement by in situ micronization of poorly water-soluble drugs. Pharmaceutical research. 2002;19(12):1894-900.
10. Vogt M, Kunath K, Dressman JB. Dissolution enhancement of fenofibrate by micronization, cogrinding and spray-drying: comparison with commercial preparations. European Journal of Pharmaceutics and Biopharmaceutics. 2008;68(2):283-8.
11. Han H-K, Choi H-K. Improved absorption of meloxicam via salt formation with ethanolamines. European journal of pharmaceutics and biopharmaceutics. 2007;65(1):99-103.
12. O'Connor KM, Corrigan OI. Comparison of the physicochemical properties of the N-(2-hydroxyethyl) pyrrolidine, diethylamine and sodium salt forms of diclofenac. International journal of pharmaceutics. 2001;222(2):281-93.
13. Viernstein H, Weiss-Greiler P, Wolschann P. Solubility enhancement of low soluble biologically active compounds—temperature and cosolvent dependent inclusion complexation. International journal of pharmaceutics. 2003;256(1-2):85-94.
14. Blagden N, de Matas M, Gavan PT, York P. Crystal engineering of active pharmaceutical ingredients to improve solubility and dissolution rates. Advanced drug delivery reviews. 2007;59(7):617-30.
15. Balakrishnan A, Rege BD, Amidon GL, Polli JE. Surfactant-mediated dissolution: contributions of solubility enhancement and relatively low micelle diffusivity. Journal of pharmaceutical sciences. 2004;93(8):2064-75.
16. Chiou WL, Chen SJ, Athanikar N. Enhancement of dissolution rates of poorly water-soluble drugs by crystallization in aqueous surfactant solutions I: Sulfathiazole, prednisone, and chloramphenicol. Journal of pharmaceutical sciences. 1976;65(11):1702-4.
17. Abou-Taleb HA, Fathalla Z, Abdelkader H. Comparative studies of the effects of novel excipients amino acids with cyclodextrins on enhancement of dissolution and oral bioavailability of

the non-ionizable drug carbamazepine. European Journal of Pharmaceutical Sciences. 2020;155:105562.
18. Foster NR, Dehghani F, Charoenchaitrakool KM, Warwick B. Application of dense gas techniques for the production of fine particles. AAPS PharmSci. 2003;5(2):32-8.
19. Jung J, Perrut M. Particle design using supercritical fluids: literature and patent survey. The Journal of supercritical fluids. 2001;20(3):179-219.
20. Del Valle EM. Cyclodextrins and their uses: a review. Process biochemistry. 2004;39(9):1033-46.
21. Eastburn SD, Tao BY. Applications of modified cyclodextrins. Biotechnology advances. 1994;12(2):325-39.
22. Hedges AR. Industrial applications of cyclodextrins. Chemical reviews. 1998;98(5):2035-44.
23. Lu X, Chen Y. Chiral separation of amino acids derivatized with fluoresceine-5-isothiocyanate by capillary electrophoresis and laser-induced fluorescence detection using mixed selectors of β-cyclodextrin and sodium taurocholate. Journal of Chromatography A. 2002;955(1):133-40.
24. Baudin C, Pean C, Perly B, Gosselin P. Inclusion of organic pollutants in cyclodextrins and derivatives. International Journal of Environmental Analytical Chemistry. 2000;77(3):233-42.
25. Kumar R, Dahiya J, Singh D, Nigam P. Biotransformation of cholesterol using Lactobacillus bulgaricus in a glucose-controlled bioreactor. Bioresource technology. 2001;78(2):209-11.
26. Koukiekolo R, Desseaux V, Moreau Y, Marchis-Mouren G, Santimone M. Mechanism of porcine pancreatic α-amylase: Inhibition of amylose and maltopentaose hydrolysis by α-, β-and γ-cyclodextrins. European journal of biochemistry. 2001;268(3):841-8.
27. Selvan GT, Poomalai S, Ramasamy S, Selvakumar PM, Muthu Vijayan Enoch IV, Lanas SG, et al. Differential metal ion sensing by an antipyrine derivative in aqueous and β-cyclodextrin media: selectivity tuning by β-cyclodextrin. Analytical chemistry. 2018;90(22):13607-15.
28. Chandrasekaran S, Sameena Y, Enoch IV. Modulation of the interaction of Coumarin 7 with DNA by β-cyclodextrin. Journal of Inclusion Phenomena and Macrocyclic Chemistry. 2015;81(1):225-36.
29. Sudha N, Enoch I. Interaction of curculigosides and their β-cyclodextrin complexes with bovine serum albumin: a fluorescence spectroscopic study. Journal of solution chemistry. 2011;40(10):1755-68.
30. Enoch I, Swaminathan M. Stoichiometrically different inclusion complexes of 2-aminofluorene and 2-amino-9-hydroxyfluorene in β-cyclodextrin: a spectrofluorimetric study. Journal of Fluorescence. 2006;16(5):697-704.
31. Becket G, Schep LJ, Tan MY. Improvement of the in vitro dissolution of praziquantel by complexation with α-, β-and γ-cyclodextrins. International journal of pharmaceutics. 1999;179(1):65-71.
32. Szente L, Szejtli J. Highly soluble cyclodextrin derivatives: chemistry, properties, and trends in development. Advanced drug delivery reviews. 1999;36(1):17-28.
33. Lindberg B, Lindberg J, Pitha J, Rao CT, Harata K. Synthesis of some 2-O-(2-hydroxyalkyl) and 2-O-(2, 3-dihydroxyalkyl) derivatives of cyclomaltoheptaose. Carbohydrate research. 1991;222:113-9.
34. Jambhekar S, Casella R, Maher T. The physicochemical characteristics and bioavailability of indomethacin from β-cyclodextrin, hydroxyethyl-β-cyclodextrin, and hydroxypropyl-β-cyclodextrin complexes. International journal of pharmaceutics. 2004;270(1-2):149-66.
35. Manosroi J, Apriyani MG, Foe K, Manosroi A. Enhancement of the release of azelaic acid through the synthetic membranes by inclusion complex formation with hydroxypropyl-β-cyclodextrin. International journal of pharmaceutics. 2005;293(1-2):235-40.

36. Wenz G, Höfler T. Synthesis of highly water-soluble cyclodextrin sulfonates by addition of hydrogen sulfite to cyclodextrin allyl ethers. Carbohydrate research. 1999;322(3-4):153-65.
37. Shuang S, Choi MM. Retention behaviour and fluorimetric detection of procaine hydrochloride using carboxymethyl-β-cyclodextrin as an additive in reversed-phase liquid chromatography. Journal of Chromatography A. 2001;919(2):321-9.
38. Abdelkader H, Fatease AA, Fathalla Z, Shoman ME, Abou-Taleb HA, Abourehab MA. Design, Preparation and Evaluation of Supramolecular Complexes with Curcumin for Enhanced Cytotoxicity in Breast Cancer Cell Lines. Pharmaceutics. 2022;14(11):2283.
39. Muhrer G, Meier U, Fusaro F, Albano S, Mazzotti M. Use of compressed gas precipitation to enhance the dissolution behavior of a poorly water-soluble drug: generation of drug microparticles and drug–polymer solid dispersions. International journal of pharmaceutics. 2006;308(1-2):69-83.
40. Gwak H-S, Choi J-S, Choi H-K. Enhanced bioavailability of piroxicam via salt formation with ethanolamines. International journal of pharmaceutics. 2005;297(1-2):156-61.
41. Joshi HN, Tejwani RW, Davidovich M, Sahasrabudhe VP, Jemal M, Bathala MS, et al. Bioavailability enhancement of a poorly water-soluble drug by solid dispersion in polyethylene glycol–polysorbate 80 mixture. International journal of pharmaceutics. 2004;269(1):251-8.
42. Kennedy M, Hu J, Gao P, Li L, Ali-Reynolds A, Chal B, et al. Enhanced bioavailability of a poorly soluble VR1 antagonist using an amorphous solid dispersion approach: a case study. Molecular pharmaceutics. 2008;5(6):981-93.
43. Rincón-López J, Almanza-Arjona YC, Riascos AP, Rojas-Aguirre Y. Technological evolution of cyclodextrins in the pharmaceutical field. Journal of Drug Delivery Science and Technology. 2021;61:102156.
44. Mai NNS, Nakai R, Kawano Y, Hanawa T. Enhancing the solubility of curcumin using a solid dispersion system with hydroxypropyl-β-cyclodextrin prepared by grinding, freeze-drying, and common solvent evaporation methods. Pharmacy. 2020;8(4):203.
45. Miranda GM, Santos VORe, Bessa JR, Teles YC, Yahouedehou SCMA, Goncalves MS, et al. Inclusion complexes of non-steroidal anti-inflammatory drugs with cyclodextrins: A systematic review. Biomolecules. 2021;11(3):361.
46. Zhou J, Jia J, He J, Li J, Cai J. Cyclodextrin Inclusion Complexes and Their Application in Food Safety Analysis: Recent Developments and Future Prospects. Foods. 2022;11(23):3871.
47. Loftsson T, Brewster ME. Cyclodextrins as functional excipients: methods to enhance complexation efficiency. Journal of pharmaceutical sciences. 2012;101(9):3019-32.
48. Trott O, Olson AJ. AutoDock Vina: improving the speed and accuracy of docking with a new scoring function, efficient optimization, and multithreading. Journal of computational chemistry. 2010;31(2):455-61.
49. Sherje AP, Kulkarni V, Murahari M, Nayak UY, Bhat P, Suvarna V, et al. Inclusion complexation of etodolac with hydroxypropyl-beta-cyclodextrin and auxiliary agents: formulation characterization and molecular modeling studies. Molecular pharmaceutics. 2017;14(4):1231-42.
50. Magnusdottir A, Másson M, Loftsson T. Self association and cyclodextrin solubilization of NSAIDs. Journal of inclusion phenomena and macrocyclic chemistry. 2002;44(1-4):213-8.
51. Salah S, Mahmoud AA, Kamel AO. Etodolac transdermal cubosomes for the treatment of rheumatoid arthritis: ex vivo permeation and in vivo pharmacokinetic studies. Drug delivery. 2017;24(1):846-56.
52. Veiga MD, Díaz PJ, Ahsan F. Interactions of griseofulvin with cyclodextrins in solid binary systems. Journal of pharmaceutical sciences. 1998;87(7):891-900.
53. Neacșu A. Physicochemical investigation of the complexation between γ-cyclodextrin and doxorubicin in solution and in solid state. Thermochimica Acta. 2018;661:51-8.
54. Pralhad T, Rajendrakumar K. Study of freeze-dried quercetin–cyclodextrin binary systems by DSC, FT-IR, X-ray diffraction and SEM analysis. Journal of pharmaceutical and biomedical analysis. 2004;34(2):333-9.

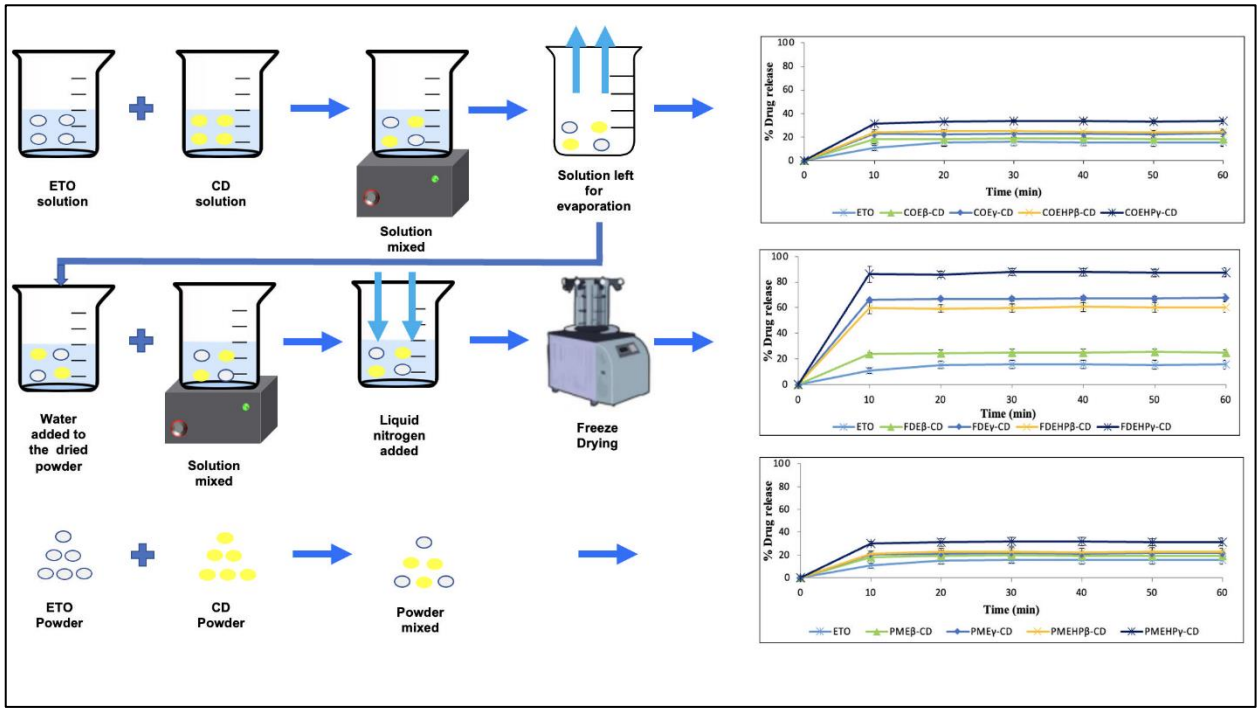

Graphical abstract: Effect of the preparation method of ETO with CDs on the dissolution profile.